

Fig. 1. (a) Trends (sketch) for I_{th} vs V_{sd} in the Kondo regime for several B . $(\partial I_{th}/\partial V_{sd})|_{V_{sd}=0}$ is a universal function of B/T_K and changes sign (“kink”) at a universal field $B = B_{th} = B_c$ [see Fig. 4(a)], while $I_{th}(V_{sd} = 0)$ [33] changes sign at $B = B_0 > B_c$ and is non-universal [see Fig. 4(a), Ref. 34 and Sec. SM.3.5.5 in Supplemental Material [25]]. (b) Asymmetric molecular junction consisting of a NNR molecule anchored to source/drain leads. (c) Anderson model of the molecule in (b) in a magnetic field B . A singly occupied level ϵ_0 with Coulomb repulsion U and gate voltage $V_g = (\epsilon_0 + U/2)/\Gamma$ coupled to hot/cold source/drain leads with strength $\Gamma = \Gamma_s + \Gamma_d$ gives rise to a spin-1/2 Kondo effect for $V_g \approx 0$ resulting in an increase of spectral weight (Kondo resonance) at the Fermi energy, E_F . The field B splits the up/down levels at ϵ_0 by $g\mu_B B$ and the Kondo resonance in dI/dV_{sd} by $2g\mu_B B$ [35, 36] (for $g\mu_B B \gg k_B T_K$). A thermal bias $\Delta T > 0$ causes a thermocurrent I_{th} to flow between source and drain, measured as described in (d). (d) False-coloured scanning electron microscopy image of the thermoelectric device. Bias and thermal voltages are generated by a DC+AC bias voltage source, $V_{sd} + \tilde{V}_{sd}(\omega_1)$, and a AC heater current source, $\tilde{I}_h(\omega_2)$, on the hot left lead. The resulting DC, AC electrical currents and AC thermocurrent, I_{sd} , $\tilde{I}_{sd}(\omega_1)$ and $\tilde{I}_{th}(2\omega_2)$, are measured simultaneously on the cold right lead.

mocurrent spectroscopy [37]. We experimentally show that the thermocurrent, I_{th} , of a molecular quantum dot in the Kondo regime exhibits a clear feature as a function of magnetic field, in the form of a zero-bias ($V_{sd} = 0$) kink appearing for fields B larger than a certain value, which we denote by B_{th} . We explain this behavior within higher-order Fermi-liquid theory [22, 24] for $V_{sd} \ll T_K$, and an approximate nonequilibrium Green function approach [38] for $V_{sd} \gtrsim T_K$. Within the former, to leading order in V_{sd}, T and ΔT , where ΔT is the applied thermal-bias, we find in the low-temperature strong-coupling regime $\Delta T \ll T \ll T_K$,

$$I_{th}(T, V_{sd}) = \gamma \frac{\pi^2 k_B}{3} T \Delta T [s_0(B) + s_1(B) V_{sd}], \quad (2)$$

where the constant γ and the coefficients $s_0(B)$ and $s_1(B)$ are given in Ref. 25. Remarkably, we show that, (i), $s_1(B)/s_1(0)$ and $c_V(B)/c_V(0)$ are described by essentially the same universal scaling function in the Kondo

regime, showing that the zero-bias thermocurrent slope [$\propto s_1(B)$] probes magnetic field universality, and, (ii), B_{th} coincides with B_c , thus demonstrating that thermocurrent spectroscopy provides a new route to directly probe the splitting of the Kondo resonance [28] and extract the universal field $B_c = B_{th}$. Our findings are concisely summarized in the sketch in Fig. 1(a). We note, that in contrast to the zero-bias thermocurrent slope, the zero-bias thermocurrent, $I_{th}(T, V_{sd} = 0)$ [$\propto s_0(B)$], measured in Ref. 33 as a function of gate-voltage (V_g) and magnetic field and found to change sign at a certain field B_0 , is nonuniversal [Fig. 4(a), Ref. 34 and Sec. SM.3.5.5 of Supplemental Material [25]]. Thus $I_{th}(T, V_{sd} = 0)$ does not provide a hallmark for the splitting of the Kondo resonance and cannot be used to extract B_c , in contrast to the thermocurrent spectroscopy proposed in this Letter [which measures also $s_1(B)$].

Experiment and results.— The experiment is carried out on a molecular quantum dot consisting of an organic

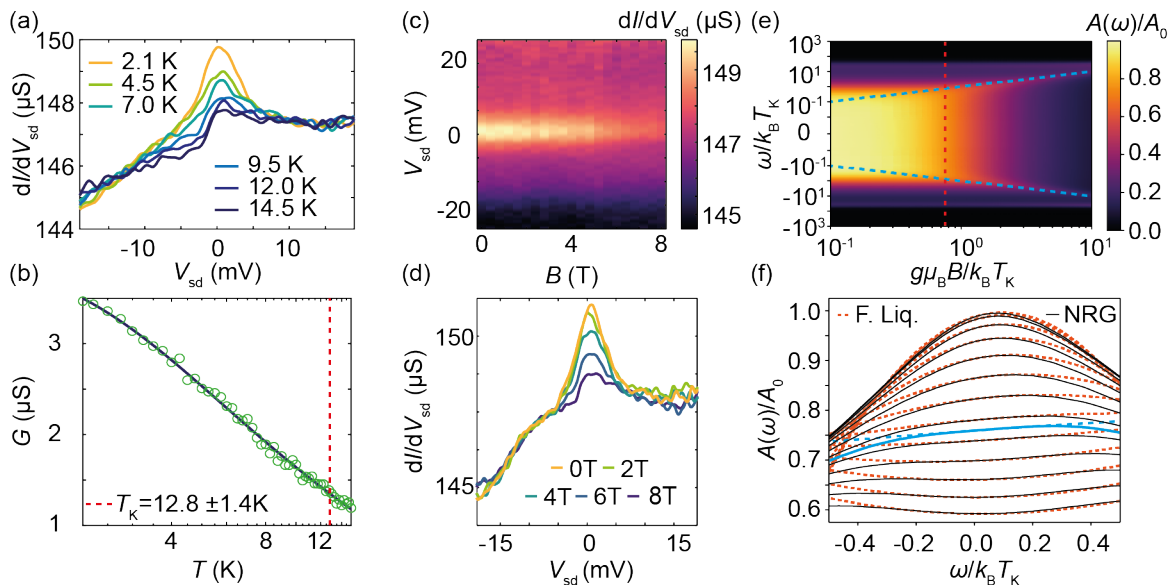


Fig. 2. (a) Differential conductance, dI/dV_{sd} , of the molecular quantum dot vs V_{sd} at different temperatures. (b) Peak conductances of Kondo resonance vs temperature and fit to a spin-1/2 Kondo model yielding $T_K \approx 12.8$ K. (c)-(d) Experimental dI/dV_{sd} vs V_{sd} at different magnetic fields. (e) NRG Spectral function $A(\omega)/A_0$ with $A_0 = 1/2\pi\Gamma$ of the Anderson model vs energy (ω) at different magnetic fields for $V_g = (\epsilon_0 + U/2)/\Gamma = -1$ and $U/\Gamma = 8$. Vertical dashed line: splitting field $g\mu_B B/k_B T_K = g\mu_B B_c/k_B T_K = 0.75$, blue dashed lines $[\omega(B) = \pm g\mu_B B]$ indicate the position of the split Kondo peaks in $A(\omega)$ for $B \gg B_c$ [35, 36]. (f) $A(\omega)/A_0$ from line cuts in (e) at $g\mu_B B/k_B T_K = 0, 0.1, \dots, 0.7, 0.75, 0.8, \dots, 1.2$ (solid lines), compared to $A(\omega)/A_0$ from higher-order Fermi-liquid theory (dashed lines). Blue lines indicate the precise splitting field $B = B_c$. A g -factor of $g = 2$ is used, as measured by electron paramagnetic resonance (Sec. SM.4.2 of Supplemental Material [25]).

radical molecule (nitronyl nitroxide radical, NNR) made up of a backbone and a nitronyl-nitroxide side group where an unpaired electron resides as shown in Fig. 1(b). Such free radical molecules are model systems to study the spin-1/2 Kondo effect [Fig. 1(c)] [39–41]. Furthermore, their asymmetric structure and the additional pyridine anchoring sites allow to achieve asymmetric and strong-coupling between the source/drain leads and the molecule (quantified by the tunnel coupling strengths Γ_s and Γ_d , Fig 1(b)). We form a NNR-molecule quantum dot in the thermoelectric device shown in Fig. 1(d) by immersing electromigrated nanogaps in the molecular solution [42]. The thermoelectric device incorporates a local backgate and two micro-heaters in direct thermal contact with the source/drain leads [see Fig. 1(d) and Sec. SM.1.1 in Supplemental Material [25]].

Evidence for a Kondo effect is shown by the strong suppression of the zero-bias peak in the measured dI/dV_{sd} , both as a function of increasing T [Fig. 2(a)-2(b)] and B [Fig. 2(c)-2(d)]. The T -dependence of the zero-bias peak height [Fig. 2(b)] is well described by the numerical renormalization group (NRG) conductance of a spin-1/2 Kondo model and yields $T_K = 12.8$ K (Sec. SM.1.3 in Supplemental Material [25]). In addition, based on the structure of the molecule, an asymmetric coupling is expected. Assuming, $\Gamma_d \gg \Gamma_s$ (see Sec. SM.3.5.6 of Supplemental Material [25] for the opposite case), we

find $\Gamma_s/\Gamma_d \approx 0.017$. An underscreened Kondo effect [18, 19], requiring a larger molecular spin ($S > 1/2$), is excluded in our case, since such an effect would result in a split Kondo resonance in dI/dV_{sd} starting already at zero field, which is not observed in Fig. 2(c)-2(d). Thus, a single-level Anderson model describing a $S = 1/2$ Kondo effect [Fig. 1(c)] is justified by the data. In the rest of this Letter, the base temperature of the quantum dot is kept at $T \approx 2$ K $\ll T_K$ while the thermocurrent is measured for a small thermal bias $\Delta T \approx 0.6$ K $\ll T \ll T_K$ so that we probe the strongly-coupled Kondo regime (see Secs. SM.2.4-5 and Secs. SM.3.6.4-5 of Supplemental Material [25] for thermal bias/temperature effects).

A closer look at the magnetic field dependence of dI/dV_{sd} in Fig. 2(c)-2(d), indicates that the expected splitting of the Kondo peak at a critical field $B_c \approx 7.15$ T [43] is not observed. This is in part due to the presence of a large non-Kondo (i.e., field and temperature independent) contribution in Figs. 2(a) and 2(d) which may mask the appearance of a splitting at zero bias. In addition, the largest magnetic field used, $B = 8$ T, was only marginally larger than B_c . For a device where higher fields relative to B_c could be applied, such a splitting could be observed (Sec. SM.2.1 of Supplemental Material [25]). Despite these complicating factors in extracting B_c from dI/dV_{sd} for the particular device studied, there is also a general problem in doing so, which can best be appre-

ciated by attempting this from exact theoretical results. This is illustrated in Figs. 2(e)-2(f) which shows the spectral function $A(\omega = eV_{sd}) \sim dI/dV_{sd}$ within higher-order Fermi liquid theory and within the NRG. While the precise value of B_c from the color map (vertical dashed line) is impossible to determine visually in Fig. 2(e), it can be deduced from the line cuts in Fig. 2(f) as the field where the curvature of the spectral function at zero energy vanishes. However, such accuracy in second derivatives of $A(\omega = eV_{sd}) \sim dI/dV_{sd}$ (and third derivatives of the current) is difficult to attain from experimental data with finite error bars.

The above difficulty can be resolved via thermocurrent spectroscopy. Figs. 3(a)-3(b) show the measured thermocurrent as a function of bias voltage and magnetic field, while Fig. 3(c)-3(d) show analogous theory results within an approximate nonequilibrium Green function approach (Sec. SM.3.6 of Supplemental Material [25]). First, notice that the large non-Kondo contribution to the differential conductance [Figs. 2(a) and 2(d)], is absent in the thermocurrent Fig. 3(b), with the latter being largely symmetric in magnitude around zero bias, in agreement with theory [Fig. 3(d)]. The reason for this is that the thermocurrent essentially measures a difference of electrical currents (in the presence/absence of thermal bias), and thus filters out the non-Kondo contributions. By the same token the thermocurrent therefore probes universal aspects of Kondo physics more precisely than the differential conductance. Secondly, we now see a clear feature, in the form of a zero-bias kink with a negative slope of the thermocurrent, appearing in the thermocurrent at a field $B = B_{th}$. This is qualitatively well captured, together with the behavior at higher voltages $V_{sd} \gtrsim T_K$, by the approximate nonequilibrium Green function approach [Figs. 3(c) and 3(d)]. However, the precise field at which this feature occurs and its connection to B_c requires a more exact theory, which is provided by the higher-order Fermi-liquid theory [Eq. (2) and Sec. SM.3.5 of Supplemental Material [25]]. Preempting the result of this theory, we note that analyzing the experimental data in Figs. 3(a) and 3(b) for the slope of the thermocurrent $dI_{th}/dV_{sd}(V_{sd} = 0)$ at zero bias voltage as a function of magnetic field, we find that this slope vanishes (i.e., the kink appears) at $B_{th} \approx 6.6$ T. This value is within 10% of the expected $B_c \approx 7.15$ T and already suggests the connection of B_{th} to B_c , i.e., that $B_{th} = B_c$, and, hence, that the splitting of the Kondo resonance can be directly measured in the bias voltage dependence of $I_{th}(V_{sd})$.

Equation (2), with coefficients $s_i(B), i = 0, 1$ evaluated exactly for all magnetic fields within the NRG (Sec. SM.3.5 of Supplemental Material [25]), allows to address the experimentally observed sign change of $(\partial I_{th}(V)/\partial V_{sd})_{V=0} \propto s_1(B)$ upon increasing B above B_{th} (the "kink") and also to determine the value of B_{th} . Figure 4(a) shows the normalized zero-bias thermocur-

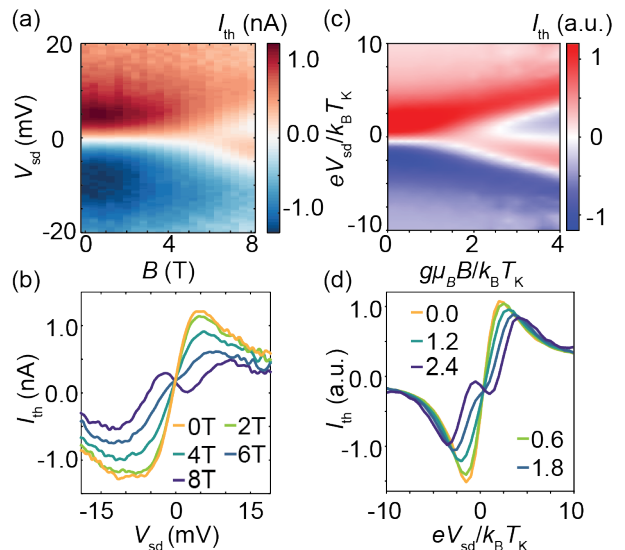


Fig. 3. (a)-(b) Measured I_{th} , vs V_{sd} at different magnetic fields. (c)-(d) Calculated I_{th} vs V_{sd} at different magnetic fields $g\mu_B B/k_B T_K$ for the Anderson model in Fig. 1(c) with $V_g = -2.5$, $U/\Gamma = 8$, $\Delta T/T_K = 0.2$ and $T/T_K = 0.5$.

rent slope $\propto s_1(B)/s_1(0)$, the normalized zero-bias thermocurrent $\propto s_0(B)/s_0(0)$ and the normalized curvature coefficient $\propto c_V(B)/c_V(0)$ as a function of magnetic field and for a range of gate voltages V_g in the Kondo regime. First, notice that both $c_V(B)/c_V(0)$ and $s_1(B)/s_1(0)$ [in contrast to $s_0(B)/s_0(0)$] are universal scaling functions of $g\mu_B B/k_B T_K$ with only a weak dependence on V_g [inset Fig. 4(a)], and while distinct, they lie within about 1% of each other [inset Fig. 4(a) and Fig. S13 of Supplemental Material [25]]. Thus, measuring the field dependence of $s_1(B)$ via thermocurrent spectroscopy, requiring only a first derivative with respect to bias-voltage, equivalently probes the magnetic field universality from an electrical conductance measurement, which, however, requires a second derivative with respect to bias-voltage and is consequently less accurate. Furthermore, since both the thermocurrent slope at $V_{sd} = 0$, and the curvature coefficient $c_V(B)$, change sign at essentially the same magnetic field, i.e., $B_{th} = B_c \approx 0.75k_B T_K/\mu_B$ (to within around 1% for all V_g in the Kondo regime), thermocurrent measurements of Kondo correlated quantum dots at finite bias voltage provide a new way to determine the splitting of the Kondo resonance via a sign change in the slope of the thermocurrent with respect to bias voltage.

In Fig. 4(b) we show a direct comparison between theory and experiment for the slope of the zero-bias thermocurrent as a function of magnetic field. The experimental data follows well the universal curve for $s_1(B)/s_1(0)$, and the aforementioned value extracted from this data for $B_{th} \approx 6.6$ T ($g\mu_B B_{th}/k_B T_K = 0.69$), is consistent with the expected splitting field of $B_{th} \approx 7.15$ T ($g\mu_B B_{th}/k_B T_K \approx 0.75$). The largest available

field, 8 T, did not allow accessing the minimum of the $s_1(B)$ vs B curve or the slow increase of $s_1(B)$ to zero at $B \gg T_K$. The agreement between theory and experiment at the largest fields measured $B > B_{\text{th}}$ is reduced, but still within the error bounds of the experimental data for all fields. The large energy level separation in a molecular quantum dot grants this good agreement between the theory and experiment, even under a simple single-level assumption in the transport window [Fig. 1(c)]. The extracted B_c from the thermocurrent validates the theory prediction with higher accuracy than has so far been reported (see Sec. SM.3.5.2 of Supplemental Material [25] for previous estimates).

Conclusion.— In summary, we have studied the effect of a magnetic field on a Kondo-correlated molecular quantum dot via non-linear thermocurrent spectroscopy. We demonstrated theoretically and confirmed experimentally, that the nonequilibrium thermocurrent, via its zero-bias slope $s_1(B)$, exhibits universal Fermi-liquid magnetic field scaling, and that the vanishing of $s_1(B)$ at $B = B_{\text{th}}$ with $B_{\text{th}} = B_c$, directly probes the splitting of the Kondo resonance. Since the thermocurrent is largely robust against parasitic conductive phenomena, it provides a more clearcut signature of this hallmark than is available from conductance measurements only. The ability to tune thermal- and voltage-bias, as well as temperature and magnetic field, opens up possibilities for using thermocurrent spectroscopy to yield insights into Kondo physics of nano-scale systems and may prompt theoretical investigations to address the largely unexplored area of nanosystems far from thermal and electrical equilibrium.

We thank J. de Bruijkere for his support in analysis software and M. van der Star for his help in sample fabrication. This work is part of the Organization for Scientific Research (NWO) and the Ministry of Education, Culture, and Science (OCW). P.G. (research associate) acknowledges financial support from the F.R.S.-FNRS of Belgium and a Marie Skłodowska-Curie Individual Fellowship under Grant TherSpinMol (ID: 748642) from the European Union's Horizon 2020 research and innovation programme. H.S.J.v.d.Z, C.H., M.M. and D.V. acknowledge funding by the EU (FET-767187-QuJET). Computing time granted through JARA on the supercomputer JURECA at Forschungszentrum Jülich is gratefully acknowledged (T.A.C.). M.M. acknowledges support from the Swiss National Science Foundation (SNF grant numbers 200020-178808) and the 111 project (90002-18011002). C.W. thanks the Independent Research Fund Denmark for an international postdoctoral grant (9059-00003B).

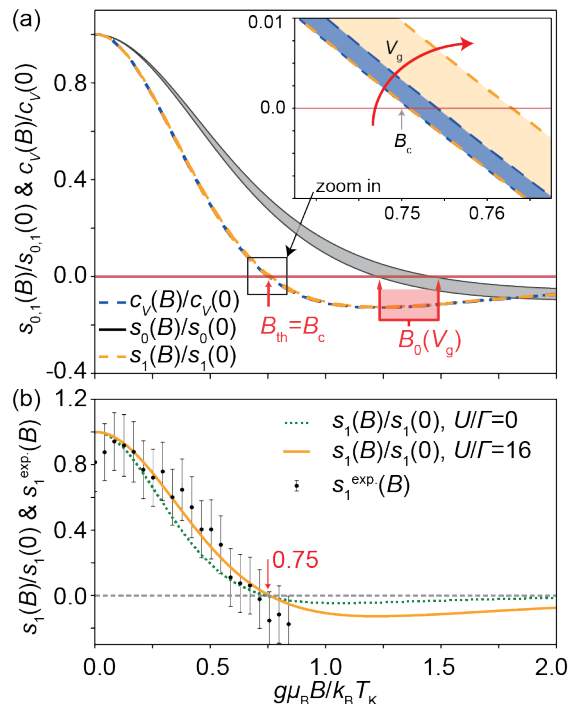


Fig. 4. (a) Calculated zero-bias normalized thermocurrent slope $s_1(B)/s_1(0)$ and normalized curvature coefficient $c_v(B)/c_v(0)$ vs $g\mu_B B/k_B T_K$, for gate voltages $1 \leq V_g = (\varepsilon_0 + U/2)/\Gamma \leq 5$ in the Kondo regime exhibiting scaling collapse [Anderson model in Fig. 1(c) with $U/\Gamma = 16$]. Also shown is the nonuniversal normalized zero-bias thermocurrent $s_0(B)/s_0(0)$ with a sign change at a strongly V_g -dependent B_0 . Inset: a close up of $c_v(B)/c_v(0)$ and $s_1(B)/s_1(0)$ in the region $B = B_{\text{th}} = B_c \approx 0.75k_B T_K/g\mu_B$ where they change sign, and their V_g -dependence. (b) Least-squares fit of the experimentally obtained zero-bias thermocurrent slope $s_1^{\text{exp}}(B)$ to the universal theory curve for $s_1(B)/s_1(0)$ in (a). Error bars denote 1σ confidence intervals (see Sec.SM.1.4 of Supplemental Material [25]). The estimated experimental $B_{\text{th}} \approx 0.69k_B T_K/g\mu_B$ is close to theory ($0.75k_B T_K/g\mu_B$). A fit of the same data to the noninteracting case with $U = 0$ and $\varepsilon_0 = -0.1\Gamma$ (green dotted line) yielded a RMS deviation that was 194% larger than for the Kondo scaling curve.

* Email: pascal.gehring@uclouvain.be

- [1] W. J. de Haas, J. de Boer, and G. J. van den Berg, *Physica* **1**, 1115 (1934).
- [2] J. Kondo, *Prog. Theor. Phys.* **32**, 37 (1964).
- [3] A. C. Hewson, *The Kondo Problem to Heavy Fermions* (Cambridge University Press, Cambridge, 1997).
- [4] A. Georges, G. Kotliar, W. Krauth, and M. J. Rozenberg, *Rev. Mod. Phys.* **68**, 13 (1996).
- [5] H. v. Löhneysen, A. Rosch, M. Vojta, and P. Wölfle, *Rev. Mod. Phys.* **79**, 1015 (2007).
- [6] D. Goldhaber-Gordon, H. Shtrikman, D. Mahalu, D. Abusch-Magder, U. Meirav, and M. A. Kastner, *Nature* **391**, 156 (1998).

- [7] S. M. Cronenwett, T. H. Oosterkamp, and L. P. Kouwenhoven, *Science* **281**, 540 (1998).
- [8] J. Park, A. N. Pasupathy, J. I. Goldsmith, C. Chang, Y. Yaish, J. R. Petta, M. Rinkoski, J. P. Sethna, H. D. Abruña, P. L. McEuen, and D. C. Ralph, *Nature* **417**, 722 (2002).
- [9] V. Madhavan, W. Chen, T. Jamneala, M. Crommie, and N. Wingreen, *Science* **280**, 567 (1998).
- [10] S. Ozaki, K. Itakura, and Y. Kuramoto, *Phys. Rev. D* **94**, 074013 (2016).
- [11] D. J. Gross and F. Wilczek, *Phys. Rev. D* **8**, 3633 (1973).
- [12] H. David Politzer, *Physics Reports* **14**, 129 (1974).
- [13] P. W. Anderson, *Journal of Physics C: Solid State Physics* **3**, 2436 (1970).
- [14] K. G. Wilson, *Rev. Mod. Phys.* **47**, 773 (1975).
- [15] N. Andrei, K. Furuya, and J. H. Lowenstein, *Rev. Mod. Phys.* **55**, 331 (1983).
- [16] D. Goldhaber-Gordon, J. Göres, M. A. Kastner, H. Shtrikman, D. Mahalu, and U. Meirav, *Phys. Rev. Lett.* **81**, 5225 (1998).
- [17] C. Gonzalez-Buxton and K. Ingersent, *Phys. Rev. B* **57**, 14254 (1998).
- [18] N. Roch, S. Florens, T. A. Costi, W. Wernsdorfer, and F. Balestro, *Phys. Rev. Lett.* **103**, 197202 (2009).
- [19] J. J. Parks, A. R. Champagne, T. A. Costi, W. W. Shum, A. N. Pasupathy, E. Neuscamman, S. Flores-Torres, P. S. Cornaglia, A. A. Aligia, C. A. Balseiro, G. K.-L. Chan, H. D. Abruña, and D. C. Ralph, *Science* **328**, 1370 (2010).
- [20] Z. Iftikhar, A. Anthore, A. K. Mitchell, F. D. Parmentier, U. Gennser, A. Ouerghi, A. Cavanna, C. Mora, P. Simon, and F. Pierre, *Science* **360**, 1315 (2018).
- [21] T. A. Costi, L. Bergqvist, A. Weichselbaum, J. von Delft, T. Micklitz, A. Rosch, P. Mavropoulos, P. H. Dederichs, F. Mallet, L. Saminadayar, and C. Bäuerle, *Phys. Rev. Lett.* **102**, 056802 (2009).
- [22] A. Oguri and A. C. Hewson, *Phys. Rev. Lett.* **120**, 126802 (2018).
- [23] A. Oguri and A. C. Hewson, *Phys. Rev. B* **97**, 035435 (2018).
- [24] M. Filippone, C. P. Moca, A. Weichselbaum, J. von Delft, and C. Mora, *Phys. Rev. B* **98**, 075404 (2018).
- [25] See Supplemental Material at [URL] for derivation of Eqs. (1) and (2), explicit expressions for $a_0(B)$, $c_T(B)$, $c(B)$, $c_V(B)$ and $s_0(B)$, $S_1(B)$, appearing therein, their evaluation, further details of the experiment, fitting procedures, synthesis and characterization, additional experimental and theory results for the thermal-bias and temperature dependence of the thermocurrent outside the Fermi-liquid regime and including Refs. [45-73].
- [26] The other terms, $a_0(B)$ and $c(B)$ in (1) depend strongly on particle-hole and/or lead coupling asymmetry and are nonuniversal functions of B/T_K .
- [27] P. Nozières, *Journal of Low Temperature Physics* **17**, 31 (1974).
- [28] T. A. Costi, *Phys. Rev. Lett.* **85**, 1504 (2000).
- [29] A. Kogan, S. Amasha, D. Goldhaber-Gordon, G. Granger, M. A. Kastner, and H. Shtrikman, *Phys. Rev. Lett.* **93**, 166602 (2004).
- [30] C. H. L. Quay, J. Cumings, S. J. Gamble, R. d. Picciotto, H. Kataura, and D. Goldhaber-Gordon, *Phys. Rev. B* **76**, 245311 (2007).
- [31] A. V. Kretinin, H. Shtrikman, D. Goldhaber-Gordon, M. Hanl, A. Weichselbaum, J. von Delft, T. Costi, and D. Mahalu, *Phys. Rev. B* **84**, 245316 (2011).
- [32] T. Hata, Y. Teratani, T. Arakawa, S. Lee, M. Ferrier, R. Deblock, R. Sakano, A. Oguri, and K. Kobayashi, *Nature Communications* **12**, 3233 (2021).
- [33] A. Svilans, M. Josefsson, A. M. Burke, S. Fahlvik, C. Thelander, H. Linke, and M. Leijnse, *Phys. Rev. Lett.* **121**, 206801 (2018).
- [34] T. A. Costi, *Phys. Rev. B* **100**, 161106 (2019).
- [35] N. S. Wingreen and Y. Meir, *Phys. Rev. B* **49**, 11040 (1994).
- [36] J. E. Moore and X.-G. Wen, *Phys. Rev. Lett.* **85**, 1722 (2000).
- [37] P. Gehring, J. K. Sowa, C. Hsu, J. de Bruijkere, M. van der Star, J. J. Le Roy, L. Bogani, E. M. Gauger, and H. S. J. van der Zant, *Nature Nanotechnology* **16**, 426 (2021).
- [38] R. Van Roermund, S.-y. Shiao, and M. Lavagna, *Physical Review B* **81**, 165115 (2010).
- [39] Y. H. Zhang, S. Kahle, T. Herden, C. Stroh, M. Mayor, U. Schlickum, M. Ternes, P. Wahl, and K. Kern, *Nature Communications* **4**, 1 (2013).
- [40] R. Frisenda, R. Gaudenzi, C. Franco, M. Mas-Torrent, C. Rovira, J. Veciana, I. Alcon, S. T. Bromley, E. Burzurí, and H. S. J. van der Zant, *Nano Letters* **15**, 3109 (2015).
- [41] R. Gaudenzi, J. de Bruijkere, D. Reta, I. d. P. R. Moreira, C. Rovira, J. Veciana, H. S. J. van der Zant, and E. Burzurí, *ACS Nano* **11**, 5879 (2017), arXiv:1805.08126.
- [42] J. de Bruijkere, P. Gehring, M. Palacios-Corella, M. Clemente-León, E. Coronado, J. Paaske, P. Hedegård, and H. S. J. van der Zant, *Phys. Rev. Lett.* **122**, 197701 (2019).
- [43] Estimated using $B_c \approx 0.5k_B T_K^{\text{HWHM}}/g\mu_B = 0.75k_B T_K/g\mu_B$ [22, 24, 28], with $T_K^{\text{HWHM}} \approx 1.5T_K$ from Sec. SM.3.2 of Supplemental Material [25], and using T_K in Fig. 2(b).